Available online at www.sciencedirect.com
ScienceDirect
C. R. Physique 7 (2006) 751–761
COMPTES RENDUS PHYSIQUE
http://france.elsevier.com/direct/COMREN/

Towards reconfigurable and cognitive communications/Vers des communications reconfigurables et cognitives

Deterministic simulation of MIMO–UWB transmission channel

Louis-Marie Aubert *, Bernard Uguen, Friedman Tchoffo Talom

IETR/INSA, UMR CNRS 6164, 20, avenue des Buttes de Coësmes, CS 14315, 35043 Rennes, France

Available online 8 September 2006

Abstract

In order to evaluate specific multiple antenna techniques in an ultra wide band context, a deterministic MIMO–UWB (Multiple Input Multiple Output – Ultra Wide Band) channel simulator has been developed. It is based on a ray tracing approach combined with frequency domain geometrical optics and uniform theory of diffraction (GO–UTD). This article presents the theoretical framework of the simulator. This framework encompasses all the channel effects including coupled antenna arrays while exhibiting the channel reciprocity property. It is adapted for both practical ray tracing implementation and digital communication channel models realization that can be used to evaluate systems' performances. The ray tracing approach provides the angle of departure and angle of arrival, which enables one to have a deeper understanding of physical phenomena involved in MIMO transmissions. ***To cite this article: L.-M. Aubert et al., C. R. Physique 7 (2006).***

Résumé

Simulation déterministe de canaux de transmission MIMO–UWB. Dans le but d'évaluer les techniques multi-antennes dans un contexte ultra large bande, un simulateur déterministe de canal MIMO–UWB (Multiple Input Multiple Output – Ultra Wide Band) a été développé. Celui-ci est basé sur un tracé de rayons associé à l'optique géométrique et la théorie uniforme de la diffraction (OG–TUD). Ce papier présente le cadre théorique sur lequel le simulateur est basé. Ce cadre théorique fait état de l'ensemble des effets du canal en incluant les antennes ainsi que leur couplage. Le formalisme adopté permet de mettre en évidence la réciprocité du canal. Ce cadre théorique est adapté aussi bien à l'implémentation du tracé de rayons qu'à la réalisation d'un modèle de canal utilisable pour l'évaluation des performances d'un système de communications numériques. L'approche par tracé de rayons permet de disposer des angles d'arrivée et de départ et d'accéder ainsi à une compréhension plus approfondie des phénomènes physiques mis en jeu dans les transmissions MIMO–UWB. ***Pour citer cet article : L.-M. Aubert et al., C. R. Physique 7 (2006).***

Keywords: UWB; MIMO; Site specific channel simulator; Ray tracing; Channel reciprocity; Coupled antenna array

Mots-clés : UWB ; MIMO ; Simulateur de canal en environnement spécifique ; Tracé de rayons ; Réciprocité du canal ; Antennes réseaux couplées

* Corresponding author.
E-mail addresses: louis-marie.aubert@insa-rennes.fr (L.-M. Aubert), bernard.uguen@insa-rennes.fr (B. Uguen), friedman.tchoffo-talom@insa-rennes.fr (F. Tchoffo Talom).

1631-0705/$ – see front matter
doi:10.1016/j.crhy.2006.07.006

1. Introduction

The UWB (Ultra Wide Band) technique is a promising way of achieving both low and very high data rate indoor communications. However, UWB systems are subject to stringent power limitations to avoid interferences with existing systems. To overcome these limitations, sophisticated cognitive detect and avoid procedures will probably be required. Moreover, MIMO (Multiple Input Multiple Output) techniques are envisioned to improve the range or the link robustness of the UWB systems [1]. The design of these two complementary techniques requires a perfect knowledge of the transmission channel. In particular, one has to model the delay and angular clusters.

For this purpose, measurements campaigns are often carried out. However, measurements campaigns require to implement considerable resources in a MIMO–UWB case. Moreover, measurements need complex procedures to extract the clusters and rays delays and further do not give a simple access to the angles of departure and the angles of arrival. In this context, deterministic simulation is an alternative solution that overcomes these difficulties while highlighting physical phenomena involved in measurements. Delays and angles of departure and arrival are naturally known thanks to ray tracing techniques. Moreover, simulations provide channel response in multiple scenarios and arbitrary geometries antenna arrays.

Our deterministic simulation tool of UWB propagation has been described in [2] and [3]. It is based on the combination of the ray tracing technique and geometrical optics with uniform theory of diffraction (GO–UTD). This kind of simulation has shown to be a very powerful technique for the SISO (Single Input Single Output) UWB channel analysis. One can see, for example, [4–6]. Considering multiple antennas applications, deterministic simulation has also been used for theoretical MIMO channel analysis in narrow band cases [7]. Henceforth it is interesting to model heterogeneous radio environments where coexist or interfere systems with various spatial and frequency diversity strategies. For this purpose it is necessary to make channel simulation tools evolve toward a general MIMO–UWB context which naturally encompasses all simpler situations.

This article presents a theoretical framework suited for ray tracing approaches which includes antennas and propagation physical behavior as in [8–10]. First, the transfer functions are computed for each ray of the channel. These ray transfer functions take into account the frequency dependency of all channel interactions including antenna with their mismatching. The overall transfer function is then obtained by a summation over all rays bearing the propagation delays. The extension toward the MIMO channel matrix is done either rigorously or approximatively. In both cases, arbitrary coupled antenna arrays can be considered. This framework has been set up in order to explicitly highlight the reciprocal nature of the either SISO or MIMO transmission channel. The last section illustrates the possibilities offered by this joint theoretical framework and simulation tool.

2. Single ray transfer function

A channel between each couple of antennas consists in a set of rays. Each ray is characterized by its transfer function. To compute this ray transfer function, the electromagnetic field associated to the ray is first evaluated on the two polarization states θ and ϕ. The antennas with their possible mismatching are then applied to obtain the final scalar ray transfer function.

2.1. Geometric conventions and notations

In a MIMO context, let a and b be two antenna arrays made up of M and N antennas, respectively. It is convenient to define three coordinate systems to characterize the 3D space: $R_g(O, \hat{\mathbf{x}}, \hat{\mathbf{y}}, \hat{\mathbf{z}})$, $R_a(A, \hat{\mathbf{x}}_a, \hat{\mathbf{y}}_a, \hat{\mathbf{z}}_a)$, and $R_b(B, \hat{\mathbf{x}}_b, \hat{\mathbf{y}}_b, \hat{\mathbf{z}}_b)$, respectively, the global coordinates system, and the two local coordinates systems associated with antenna array a and b.

For the sake of simplicity, we adopt the same notation for both a vector quantity and its associated representation in a given coordinate system. If not specified, a vector is expressed in the global coordinates system R_g. Its Cartesian representation is a (3×1) column vector.

The M-dimensional antenna array a is in the position $\mathbf{r}_a$ and defined by the $(3 \times M)$ array $\mathbf{R}_a = [\mathbf{r}_{a_1} \dots \mathbf{r}_{a_M}]$. The N-dimensional antenna array b is in the position $\mathbf{r}_b$ and defined by the $(3 \times N)$ array $\mathbf{R}_b = [\mathbf{r}_{b_1} \dots \mathbf{r}_{b_N}]$ (Fig. 1).

A ray is a 3D polyline which links either $\mathbf{r}_{a_m}$ to $\mathbf{r}_{b_n}$ or in a SISO case $\mathbf{r}_a$ to $\mathbf{r}_b$. The unitary vectors $\hat{\mathbf{s}}_{ak}$ and $\hat{\mathbf{s}}_{bk}$ define the direction of the kth ray from the position $\mathbf{r}_a$ and from the position $\mathbf{r}_b$, respectively. These two vectors define

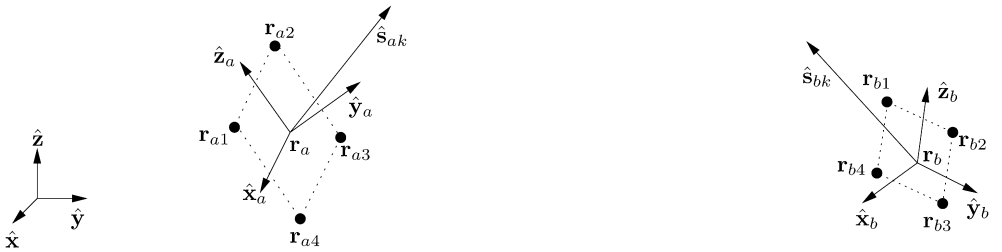

Fig. 1. Antenna arrays and coordinate systems in a 4×4 MIMO configuration.

Fig. 1. Réseaux d'antennes et repères géométriques dans une configuration MIMO 4×4.

two couples of angles (θ_{ak}, ϕ_{ak}) and (θ_{bk}, ϕ_{bk}), evaluated in the global coordinate system. The plane of departure and the plane of arrival are defined by two orthonormal bases expressed in (3×2) matrix form:

- $\mathbf{B}_{ak} = [\hat{\boldsymbol{\theta}}_{ak}\ \hat{\boldsymbol{\phi}}_{ak}]$, the basis of the plane transverse to $\hat{\mathbf{s}}_{ak}$;
- $\mathbf{B}_{bk} = [\hat{\boldsymbol{\theta}}_{bk}\ \hat{\boldsymbol{\phi}}_{bk}]$, the basis of the plane transverse to $\hat{\mathbf{s}}_{bk}$.

To retrieve the coordinates in the local bases, $\mathbf{T}_a$ and $\mathbf{T}_b$ are two (3×3) orthonormal transformation matrices:

$$\mathbf{T}_a = [\hat{\mathbf{x}}_a\ \hat{\mathbf{y}}_a\ \hat{\mathbf{z}}_a] \quad \text{and} \quad \mathbf{T}_b = [\hat{\mathbf{x}}_b\ \hat{\mathbf{y}}_b\ \hat{\mathbf{z}}_b] \tag{1}$$

Then, the Cartesian coordinates of the vectors of directions of departure or arrival expressed in the local bases are:

$$\hat{\mathbf{s}}_{ak|R_a} = \mathbf{T}_a^T \hat{\mathbf{s}}_{ak} \quad \text{and} \quad \hat{\mathbf{s}}_{bk|R_b} = \mathbf{T}_b^T \hat{\mathbf{s}}_{bk} \tag{2}$$

These directions are characterized by the couple of angles $(\theta_{ak|R_a}, \phi_{ak|R_a})$ and $(\theta_{bk|R_b}, \phi_{bk|R_b})$, which are defined on the antenna local bases. Finally, the local bases of the planes transverse to these directions are:

- $\mathbf{B}_{ak|R_a} = [\hat{\boldsymbol{\theta}}_{ak|R_a}\ \hat{\boldsymbol{\phi}}_{ak|R_a}]$, the basis of the plane transverse to $\hat{\mathbf{s}}_{ak}$ expressed in R_a;
- $\mathbf{B}_{bk|R_b} = [\hat{\boldsymbol{\theta}}_{bk|R_b}\ \hat{\boldsymbol{\phi}}_{bk|R_b}]$, the basis of the plane transverse to $\hat{\mathbf{s}}_{bk}$ expressed in R_b.

2.2. Expression of the field

The outgoing and incoming electric field expressed in the transverse planes, $\mathbf{E}_{ak}$ and $\mathbf{E}_{bk}$, are two (2×1) vectors whose elements are the $\hat{\boldsymbol{\theta}}_k$ and $\hat{\boldsymbol{\phi}}_k$ components. These fields are expressed back in the global coordinate system through the matrix product:

$$\vec{\mathbf{E}}_{ak} = \mathbf{B}_{ak}\mathbf{E}_{ak} \quad \text{and} \quad \vec{\mathbf{E}}_{bk} = \mathbf{B}_{bk}\mathbf{E}_{bk} \tag{3}$$

If the outgoing and incoming electric field are expressed in the antennas local coordinate systems as $\mathbf{E}_{ak}^{\ell}$ and $\mathbf{E}_{bk}^{\ell}$, then:

$$\vec{\mathbf{E}}_{ak|R_a} = \mathbf{B}_{ak|R_a}\mathbf{E}_{ak}^{\ell} \quad \text{and} \quad \vec{\mathbf{E}}_{bk|R_b} = \mathbf{B}_{bk|R_b}\mathbf{E}_{bk}^{\ell} \tag{4}$$

The study of the channel through the combination of a ray tracing and the GO–UTD allows us to determine the (2×2) matrices $\tilde{\mathbf{C}}_{abk}$ and $\tilde{\mathbf{C}}_{abk}^{\ell}$ which link the received incoming field to the transmitted outgoing field for each ray:

$$\mathbf{E}_{bk} = \tilde{\mathbf{C}}_{abk}\mathbf{E}_{ak} \quad \text{and} \quad \mathbf{E}_{bk}^{\ell} = \tilde{\mathbf{C}}_{abk}^{\ell}\mathbf{E}_{ak}^{\ell} \tag{5}$$

where

$$\tilde{\mathbf{C}}_{abk} = \begin{bmatrix} \tilde{C}_{abk}^{\theta\theta} & \tilde{C}_{abk}^{\theta\phi} \\ \tilde{C}_{abk}^{\phi\theta} & \tilde{C}_{abk}^{\phi\phi} \end{bmatrix} \quad \text{and} \quad \tilde{\mathbf{C}}_{abk}^{\ell} = \begin{bmatrix} \tilde{C}_{abk}^{\theta\theta\ell} & \tilde{C}_{abk}^{\theta\phi\ell} \\ \tilde{C}_{abk}^{\phi\theta\ell} & \tilde{C}_{abk}^{\phi\phi\ell} \end{bmatrix} \tag{6}$$

The tilde over $\tilde{\mathbf{C}}_{abk}$ and $\tilde{\mathbf{C}}_{abk}^{\ell}$ indicates that the propagation delay is not included in the expression. These matrices express the attenuation and the polarization transformation undergone by the ray.

2.3. The matrix ray transfer function

A ray is defined as a succession of L interactions. An interaction is a local physical effect including reflection, transmission and diffraction. The lth interaction of the kth ray is characterized by a (2×2) diagonal interaction matrix $\mathbf{A}_{lk}$:

$$\mathbf{A}_{lk} = \begin{bmatrix} A_{lk}^{\parallel} & 0 \\ 0 & A_{lk}^{\perp} \end{bmatrix} \tag{7}$$

For each interaction an incoming and an outgoing bases are also defined:

$$\mathbf{B}_{lk}^{i} = \left[\hat{\mathbf{e}}_{lk}^{i\parallel}\ \hat{\mathbf{e}}_{lk}^{i\perp}\right] \quad \text{and} \quad \mathbf{B}_{lk}^{o} = \left[\hat{\mathbf{e}}_{lk}^{o\parallel}\ \hat{\mathbf{e}}_{lk}^{o\perp}\right] \tag{8}$$

The unitary matrix linking two successive interactions on a ray is given by $\mathbf{B}_{(l-1)k}^{oT}\mathbf{B}_{lk}^{i}$. Thus, the (2×2) propagation matrix over a given ray with L interactions can be expressed as the following matrix product:

$$\tilde{\mathbf{C}}_{abk} = \mathbf{B}_{Lk}^{oT}\mathbf{B}_{bk}\left[\prod_{l=L}^{2}\mathbf{A}_{lk}\mathbf{B}_{(l-1)k}^{oT}\mathbf{B}_{lk}^{i}\right]\mathbf{A}_{1k}\mathbf{B}_{ak}^{T}\mathbf{B}_{1k}^{i} \tag{9}$$

One can notice the specific role played by only local bases associated with global coordinate system. $\tilde{\mathbf{C}}_{abk}$ does not depend on the orientation of the antennas. It stands only for the kth ray propagation channel. The ray tracing tool allows this matrix to be calculated and stored once. Then it can be used to evaluate the propagation channel for a couple of antennas whatever their orientation. The matrix $\tilde{\mathbf{C}}_{abk}^{\ell}$ expressed in the antennas local bases is then obtained from the precalculated matrix $\tilde{\mathbf{C}}_{abk}$ and antennas local bases transformation as follow:

$$\tilde{\mathbf{C}}_{abk}^{\ell} = \mathbf{B}_{bk|R_b}^{T}\mathbf{T}_{b}^{T}\mathbf{B}_{bk}\tilde{\mathbf{C}}_{abk}\mathbf{B}_{ak}^{T}\mathbf{T}_{a}\mathbf{B}_{ak|R_a} \tag{10}$$

2.4. The scalar ray transfer function

Let us define two quantities calculated for all rays which relate the antenna a in position $\mathbf{r}_a$ and the antenna b in position $\mathbf{r}_b$, in the direction of the kth ray:

$$\mathbf{F}_{ak}(f) = \sqrt{G_{ak}(f)}\,\mathbf{U}_{ak}(f) \quad \text{and} \quad \mathbf{F}_{bk}(f) = \sqrt{G_{bk}(f)}\,\mathbf{U}_{bk}(f) \tag{11}$$

where G_{ak} and G_{bk} are the gain of the antennas a and b, respectively, in the direction $\hat{\mathbf{s}}_{ak}$ and $\hat{\mathbf{s}}_{bk}$, respectively. The two (2×1) matrices $\mathbf{U}_{ak}(f)$ and $\mathbf{U}_{bk}(f)$ give the polarization state of the antennas a and b. $\mathbf{U}_{ak}(f)$ is expressed in the local basis $\mathbf{B}_{ak|R_a}$ associated with the direction of departure $\hat{\mathbf{s}}_{ak}$ with the following unitary property [11]:

$$\left|\mathbf{U}_{ak}(f)\right|^2 = \left|U_{ak}^{\theta}(f)\right|^2 + \left|U_{ak}^{\phi}(f)\right|^2 = 1 \tag{12}$$

Of course, the same properties hold for $\mathbf{U}_{bk}(f)$.

Then, the emitted electric field necessary to initiate a GO–UTD calculation is obtained from:

$$\mathbf{E}_{ak}^{\ell}(f) = \sqrt{\frac{2Z_0}{4\pi}}\left(1 - S_a(f)\right)\mathbf{F}_{ak}(f) \tag{13}$$

where Z_0 is the free space impedance and $S_a(f)$ is the scattering parameter characterizing the mismatching of the antenna a. The received voltage is obtained by the projection of the incoming electric field on the receiving antenna. Then the ray transfer function is:

$$\tilde{H}_{abk}(f) = \frac{-jc}{\sqrt{4\pi}\sqrt{2Z_0}f}\left(1 - S_b(f)\right)\mathbf{F}_{bk}^{T}(f)\mathbf{E}_{bk}^{\ell}(f) \tag{14}$$

where $S_b(f)$ is the scattering parameter of the antenna b. Finally, if we define

$$\gamma_{ab}(f) = \frac{-jc}{4\pi f}\left(1 - S_b(f)\right)\left(1 - S_a(f)\right) \quad \text{and} \quad \alpha_{abk}(f) = \mathbf{F}_{bk}^{T}\tilde{\mathbf{C}}_{abk}^{\ell}\mathbf{F}_{ak} \tag{15}$$

then, equations (14), (13) and (5) yield:

$$\tilde{H}_{abk}(f) = \gamma_{ab}(f)\alpha_{abk}(f) \tag{16}$$

We may notice that $\gamma_{ab}(f)$ does not depend on the kth ray but only on the scattering parameters of antennas at both ends.

3. Entire SISO channel

The overall channel transfer function is derived from the summation of contributions coming from each ray. The proper phase term related to the ray propagation delay is re-introduced:

$$H_{ab}(f) = \sum_{k=1}^{K} \tilde{H}_{abk}(f)\mathrm{e}^{-2j\pi f\tau_k} \tag{17}$$

$$= \gamma_{ab}(f) \sum_{k=1}^{K} \alpha_{abk}(f)\mathrm{e}^{-2j\pi f\tau_k} \tag{18}$$

This relation takes into account frequency dependencies of antennas, and to a lesser extend, of propagation through building materials. Note that these frequency variations are often legitimately neglected in narrow band situation.

In the proposed notation, antenna a is the transmitter and antenna b the receiver. If the roles of antennas are switched, the transfer function of the transmission channel becomes:

$$H_{ba}(f) = \gamma_{ba}(f) \sum_{k=1}^{K} \alpha_{bak}(f)\mathrm{e}^{-2j\pi f\tau_k} \tag{19}$$

with

$$\gamma_{ba}(f) = \gamma_{ab}(f) \quad \text{and} \quad \alpha_{bak}(f) = \alpha_{abk}(f) \tag{20}$$

We have indeed:

$$\alpha_{bak}(f) = \mathbf{F}_{ak}^{T}\tilde{\mathbf{C}}_{bak}^{\ell}\mathbf{F}_{bk} = \mathbf{F}_{bk}^{T}\tilde{\mathbf{C}}_{abk}^{\ell\,T}\mathbf{F}_{ak}$$

and

$$\tilde{\mathbf{C}}_{bak} = \mathbf{B}_{1k}^{iT}\mathbf{B}_{ak}\left[\prod_{l=2}^{L}\mathbf{A}_{lk}\mathbf{B}_{lk}^{iT}\mathbf{B}_{(l-1)k}^{o}\right]\mathbf{A}_{Lk}\mathbf{B}_{bk}^{T}\mathbf{B}_{Lk}^{o} \tag{21}$$

Knowing that matrices $\mathbf{A}_{lk}$ are symmetric ($\mathbf{A}_{lk} = \mathbf{A}_{lk}^{T}$), the transpose of $\tilde{\mathbf{C}}_{abk}$ in (9) yield the equality:

$$\tilde{\mathbf{C}}_{bak} = \tilde{\mathbf{C}}_{abk}^{T} \quad \text{and} \quad \tilde{\mathbf{C}}_{bak}^{\ell} = \tilde{\mathbf{C}}_{abk}^{\ell\,T} \tag{22}$$

which proves the second equality in (20). Thus the SISO channel reciprocity is verified:

$$H_{ba}(f) = H_{ab}(f) \tag{23}$$

4. Reciprocal MIMO channel matrix

The MIMO channel matrix can be expressed as the product of three matrices [12]:

$$\mathbf{H}_{ab}(f) = (\mathbf{I} - \mathbf{S}_b)\bar{\mathbf{H}}_{ab}(\mathbf{I} - \mathbf{S}_a) \tag{24}$$

The symmetric matrices $\mathbf{S}_a$ and $\mathbf{S}_b$ are the scattering matrices that characterize both the mismatching and the coupling between elements of arrays a and b. If coupling at both extremities is neglected and the antennas mismatching alone is considered, S-matrices $\mathbf{S}_a$ and $\mathbf{S}_b$ are diagonal.

Two methods can be used to compute the MIMO channel matrix $\bar{\mathbf{H}}_{ab}$: a rigorous one, and an approximated one that benefits from the knowledge of angle of departure and arrival. Both these methods satisfy the reciprocity principle.

Theoretically, each term (n, m) of the $(N \times M)$ MIMO channel matrix is a different SISO channel between the antenna a_m and the antenna b_n:

$$\bar{\mathbf{H}}_{ab}(f) = \begin{bmatrix} \bar{H}_{a_1b_1}(f) & \bar{H}_{a_2b_1}(f) & \dots & \bar{H}_{a_Mb_1}(f) \\ \bar{H}_{a_1b_2}(f) & \bar{H}_{a_2b_2}(f) & \dots & \bar{H}_{a_Mb_2}(f) \\ \vdots & \vdots & \ddots & \vdots \\ \bar{H}_{a_1b_N}(f) & \bar{H}_{a_2b_N}(f) & \dots & \bar{H}_{a_Mb_N}(f) \end{bmatrix} \tag{25}$$

with

$$\bar{H}_{a_mb_n}(f) = \frac{-jc}{4\pi f} \sum_{k=1}^{K} \alpha_{a_mb_nk}(f) \mathrm{e}^{-2j\pi f \tau_{a_mb_nk}} \quad \text{and} \quad \alpha_{a_mb_nk}(f) = \mathbf{F}^T_{b_{mn}k} \tilde{\mathbf{C}}^{\ell}_{a_mb_nk} \mathbf{F}_{a_{mn}k} \tag{26}$$

where $\mathbf{F}_{a_{mn}k}$ (resp. $\mathbf{F}_{b_{mn}k}$) characterizes the antenna a_m (resp. b_n) in the direction of the kth ray linking antennas a_m and b_n.

Whereas there was previously one transfer function per ray, there are now NM different transfer functions which each requiring a specific depolarization matrix and antennas termination. Fortunately, in many practical cases it is possible to consider that ray directions are parallel on all the antennas of a same array both at the transmitter and the receiver side:

$$\hat{\mathbf{s}}_{a_{mn}k} = \hat{\mathbf{s}}_{ak} \quad \text{and} \quad \hat{\mathbf{s}}_{b_{mn}k} = \hat{\mathbf{s}}_{bk} \tag{27}$$

Then, for each ray two steering column vectors determine the phase shift between the center of the array $\mathbf{r}_a$ or $\mathbf{r}_b$ and any elements of the array $\mathbf{r}_{a_m}, \forall m \in \{1, \dots, M\}$ or $\mathbf{r}_{b_n}, \ \forall n \in \{1, \dots, N\}$:

$$\Psi_{ak}(f) = \left[\mathrm{e}^{-\frac{2j\pi f}{c}\hat{\mathbf{s}}_{ak}.(\mathbf{r}_{a_1}-\mathbf{r}_a)} \dots \mathrm{e}^{-\frac{2j\pi f}{c}\hat{\mathbf{s}}_{ak}.(\mathbf{r}_{a_M}-\mathbf{r}_a)}\right]^T \tag{28}$$

$$\Psi_{bk}(f) = \left[\mathrm{e}^{-\frac{2j\pi f}{c}\hat{\mathbf{s}}_{bk}.(\mathbf{r}_{b_1}-\mathbf{r}_b)} \dots \mathrm{e}^{-\frac{2j\pi f}{c}\hat{\mathbf{s}}_{bk}.(\mathbf{r}_{b_N}-\mathbf{r}_b)}\right]^T \tag{29}$$

Finally, the approximated MIMO channel matrix is calculated from the sole transfer function of the channel between the centers of the arrays a and b. It is noted $\mathbf{H_{ab}}(f)$ where the subscripts **a** and **b** are in bold to emphasize the fact that the matrix is build from steering vectors:

$$\mathbf{H_{ab}}(f) = \frac{-jc}{4\pi f} \sum_{k=1}^{K} \alpha_{abk}(f) \Psi^T_{bk}(f) \Psi_{ak}(f) \mathrm{e}^{-2j\pi f \tau_{abk}} \tag{30}$$

This approach implies that every antenna, at the transmitter or at the receiver, has the same radiation pattern. Thus this approach does not allow one to take into account the pattern diversity provided by coupling between antennas.

5. Illustrations

The following illustrations are obtained with the deterministic UWB channel simulator described in [2] and [3]. This simulator computes indoor channel model thanks to a 3D ray tracing technique (Fig. 2). A first comparison of results coming from simulation and measurement can be found in [13] and confirms the great potential of the simulation to characterize the channel.

Without any antennas, the simulator gives access to the $\tilde{\mathbf{C}}_{abk}(f)$ matrices of Eq. (6) and the corresponding delays τ_{abk} for all rays. The matrices $\mathbf{C}_{abk}(\tau)$ are the time domain representation of $\tilde{\mathbf{C}}_{abk}(f)$ into which delays are put back. To see the evolution of the four terms of the matrix $\mathbf{C}_{abk}(\tau)$ according to the ray, each polarization couple from all the different directions are projected on a same time axis. Fig. 3 shows this representation in the line of sight SISO configuration of Fig. 2.

Each ray is associated with an angle of departure and an angle of arrival so that the antenna can be applied properly as in Eqs. (15), (16). Subsequently, two types of antennas are considered: omnidirectional monocone antennas (Fig. 4(a)) and horn antennas (Fig. 4(b)). In both cases, antennas are rigorously introduced with their complex pattern (11) acquired from measurements in a SATIMO near field chamber (Fig. 4(c)).

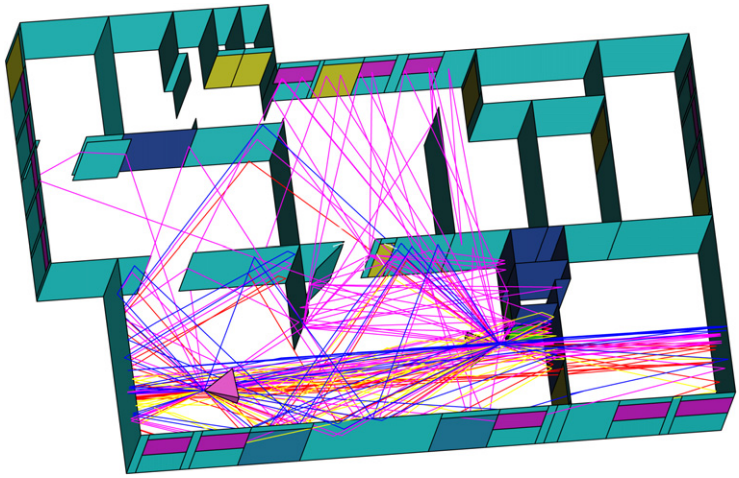

Fig. 2. 3D ray tracing in typical indoor environment.

Fig. 2. Tracé de rayons 3D dans environnement *indoor* typique.

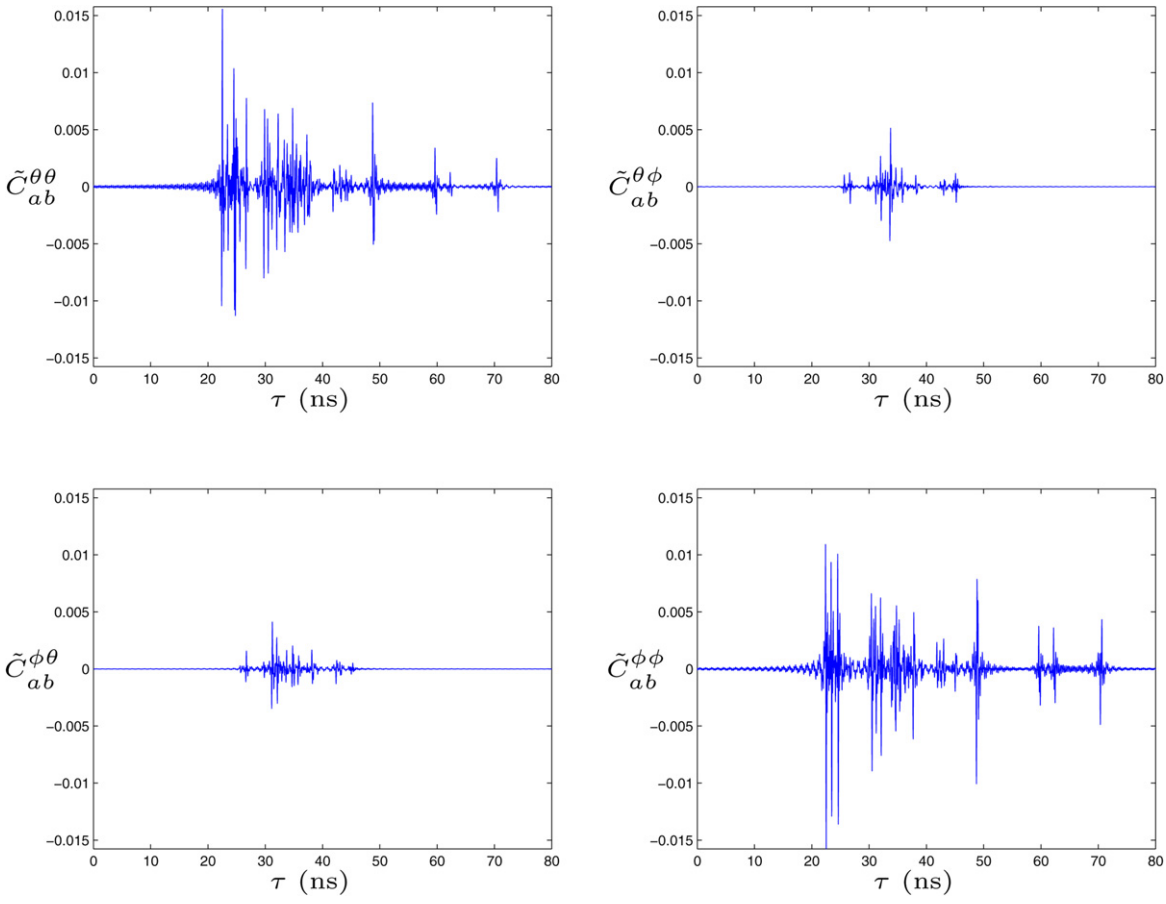

Fig. 3. Channel matrix $\mathbf{C}_{ab}(\tau)$.

Fig. 3. Matrice de canal $\mathbf{C}_{ab}(\tau)$.

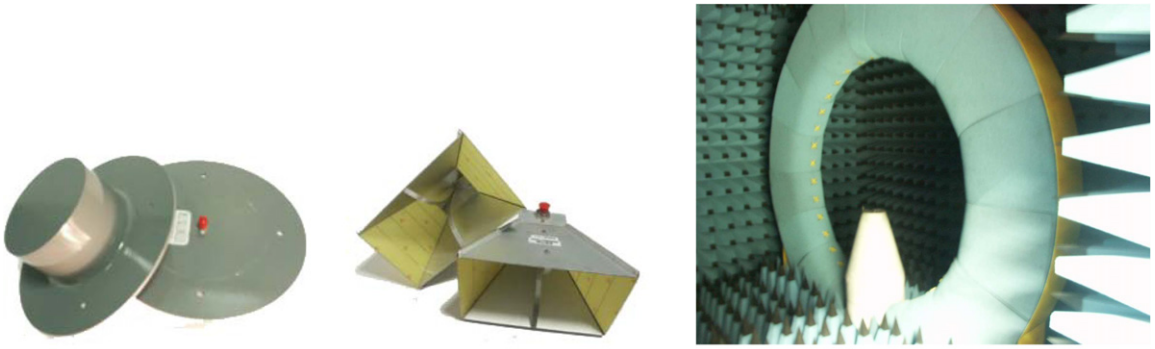

Fig. 4. Antennas measured in near field chamber: (a) omnidirectional monocone, (b) horn, (c) SATIMO near field chamber.

Fig. 4. Antennes mesurées en base champ proche : (a) monocône omnidirectionnel, (b) cornet, (c) base champ proche SATIMO.

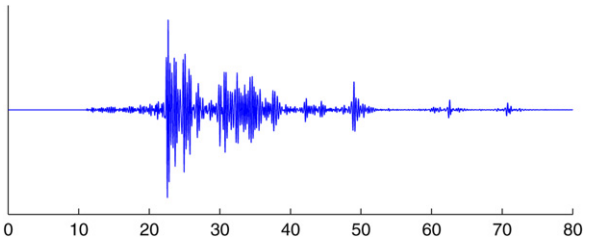

Fig. 5. Time response of the channel including omnidirectional antennas.

Fig. 5. Réponse temporelle du canal incluant les antennes omnidirectionnelles.

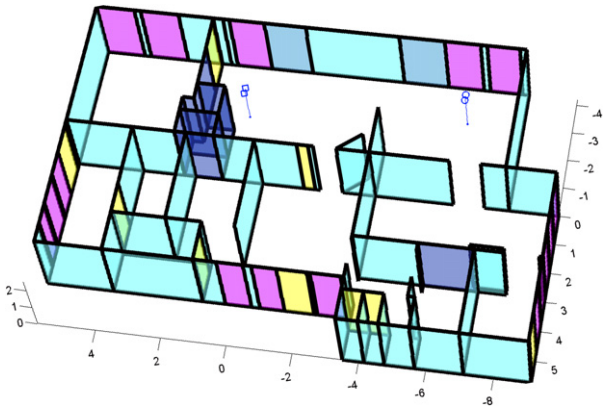

Fig. 6. Configuration of a 2×2 MIMO link.

Fig. 6. Configuration d'une liaison MIMO 2×2.

Fig. 5 depicts the signal obtained with UWB omnidirectional monocone antennas at both transmission and reception side. In this example, the channel transfer function $H_{ab}(f)$ (17) is excited by a Gaussian pulse with center frequency at 4 GHz and bandwidth equals to 2 GHz at -10 dB.

In order to have a simple representation of a multi-antennas configuration, we consider a (2×2) MIMO system in which the two transmit antennas and the two receive antennas are spaced by 15 cm (Fig. 6). Let us point out that the size and the geometry of antenna arrays are not here a limiting factor, as opposed to measurements.

Both rigorous and approximate approaches described in Section 4 are implemented in the simulator.

On the one hand, the channel matrix expressed in Eq. (24) is computed through the simulation of one ray tracing per receiving antenna. Fig. 7 represents the corresponding time domain responses to a Gaussian pulse, with the omni-

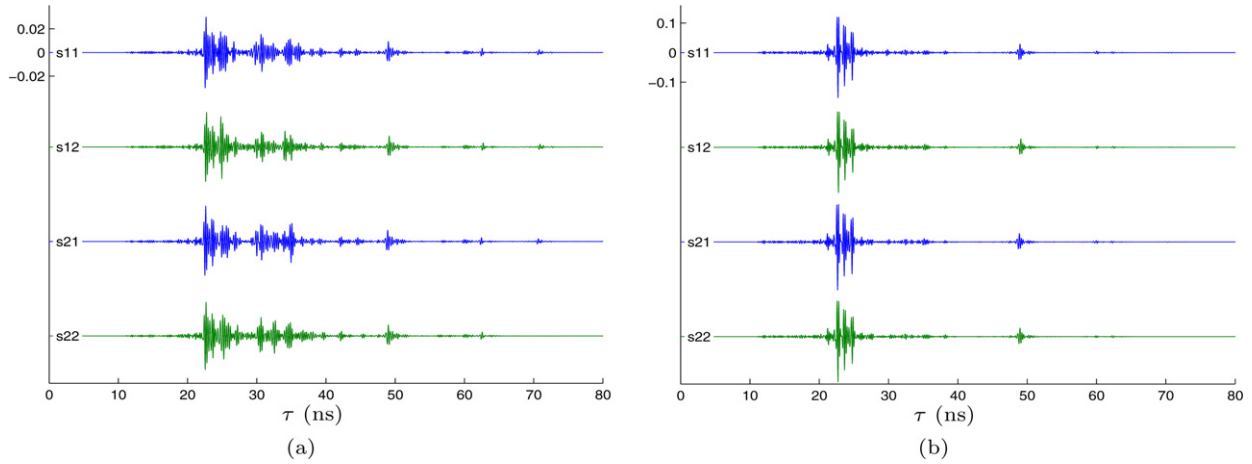

Fig. 7. (2 × 2) MIMO–UWB channel matrix in time domain with the rigorous approach: (a) omnidirectional monocone antennas, (b) horn antennas.

Fig. 7. Matrice de canal MIMO–UWB (2 × 2) dans le domaine temporel obtenue par la méthode rigoureuse : (a) antennes monocônes omnidirectionnelles, (b) antennes cornets.

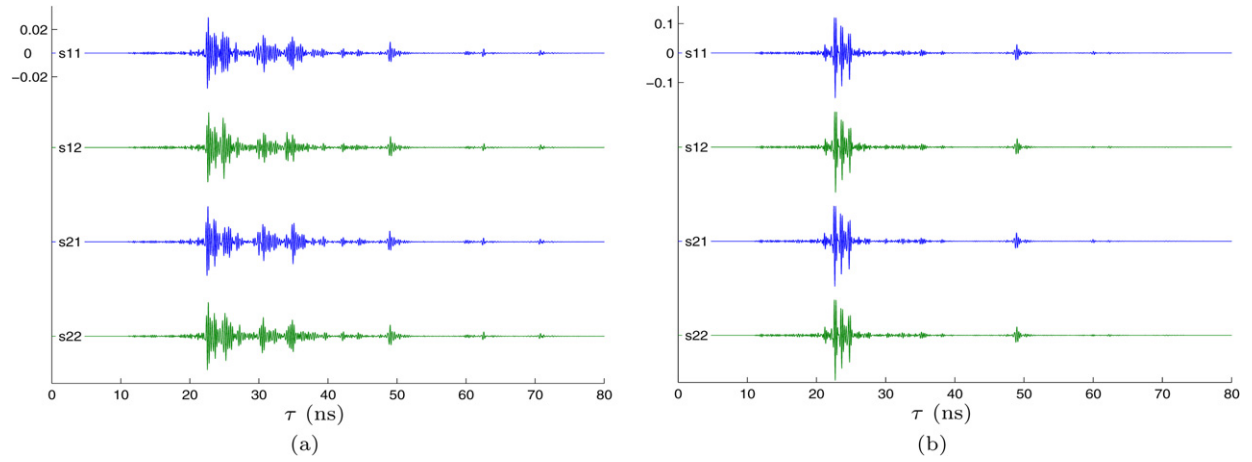

Fig. 8. (2 × 2) MIMO–UWB channel matrix in time domain with the approximate approach: (a) omnidirectional monocone antennas, (b) horn antennas.

Fig. 8. Matrice de canal MIMO–UWB (2 × 2) dans le domaine temporel obtenue par la méthode approchée : (a) antennes monocônes omnidirectionnelles, (b) antennes cornets.

directional monocone antennas (Fig. 4(a)) and the horn antennas (Fig. 4(b)). No coupling between arrays' elements is considered in these simulations.

On the other hand, one can use the approximation expressed in Eq. (30). Then, only one ray tracing is computed and the responses on each antenna are derived from the steering vectors of Eqs. (28) and (29). Fig. 8 shows the time domain response with the omnidirectional monocone antennas and the horn antennas.

Three remarks can be made on Figs. 7 and 8.

Firstly and obviously, the antenna directivity plays an important role on the channel response. Thanks to the deterministic tool, it is possible to evaluate this effect and its consequences on the statistical properties of the channel (power delay profile, delay spread, angular spread, ...).

Secondly, one can observe in Figs. 7 and 8 that time domain responses on the four channels are highly correlated. Differences between responses are negligible when antennas are directive. Rays that introduce important phase differences between elements of the array are indeed filtered by the antennas.

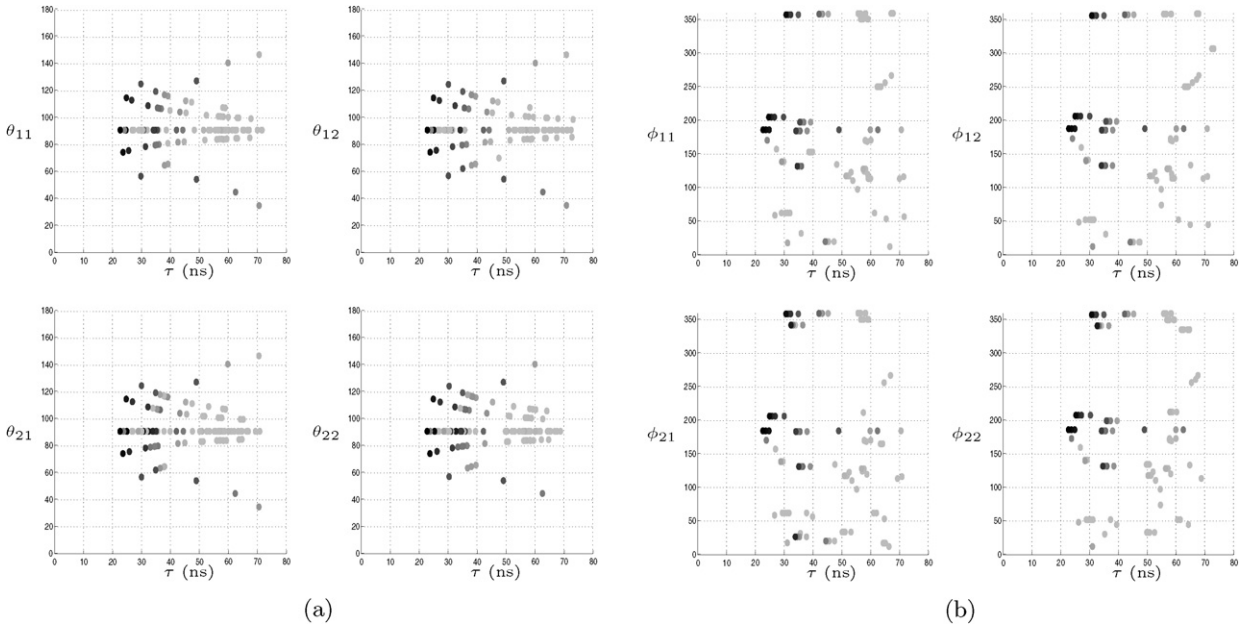

Fig. 9. Angles of arrival of rays (a) θ: elevation (b) ϕ: azimuth.

Fig. 9. Angles d'arrivée des rayons (a) θ : élévation, (b) ϕ : azimut.

Finally, a close examination of the responses provided by the two approaches, rigorous and approximate, shows that the diversity between multiple responses is slightly greater in the rigorous approach. The approximate approach is, however, justified. It consists in simulating only one channel realization, and hence is MN time faster. Therefore, one can foresee efficient techniques to built dynamic channel model where a moving path has to be sampled. Note that in this case it is necessary to define the correlation beyond which a new ray tracing has to be made.

The observation of time domain signals is enriched by the observation of angles of arrival plotted on Fig. 9. The similarity between the repartition of angles of arrival from one term of the MIMO matrix to another confirms the validity of the approximate method that relies on the hypothesis of parallel directions. The comparison of Figs. 9(a) and (b) shows that the repartition of angles of arrival is different on the two planes, vertical and horizontal. In the vertical plane, one can clearly distinguish a structure resulting of the main reflexions on floor and ceiling. Note that this observation requires a fine angular resolution which cannot be easily reached by measurements. In the horizontal plane, no clear structure appears. Nevertheless, angles close to 0 and 360°, corresponding to the backward radiation, are over represented. In this case, the uniform distribution model is not the most accurate one. A statistical study over a great number of realizations is therefore necessary.

6. Conclusion

Deterministic simulations of the channel give the possibility to lead a complementary analysis of the MIMO–UWB channel with respect to measurements. Firstly, this paper has presented the theoretical framework on which relies the deterministic modeling of the MIMO–UWB channel, based on a ray tracing method. This framework satisfies the channel reciprocity principle that is a prerequisite for time reversal communications [14,15]. Secondly, illustrations gotten from simulations have been briefly analyzed. As a conclusion of this first analysis, it seems necessary to evaluate the spatial diversity gain while the system benefits from most of the frequency diversity otherwise. Spatial correlation between UWB signal is indeed important since the fading is already softened by UWB techniques. We can expect to have to space elements of the arrays by a greater distance than in a narrow band system to benefit from the spatial diversity in a UWB case.

References

[1] A. Sibille, Time-domain diversity in ultra-wideband MIMO communications, EURASIP Journal on Applied Signal Processing 2005 (3) (March 2005) 316–327.
[2] B. Uguen, E. Plouhinec, Y. Lostanlen, G. Chassay, Deterministic ultra wideband channel modelling, in: IEEE UWBST'02, 2002.
[3] F. Tchoffo Talom, B. Uguen, E. Plouhinec, G. Chassay, A site-specific tool for UWB channel modelling, in: Joint IWUWBS and UWBST 2004 Conf., 2004.
[4] R. Yao, G. Gao, Z. Chen, W. Zhu, UWB multipath channel model based on time-domain UTD technique, in: IEEE Global Telecommunications Conference GLOBECOM '03, 2003.
[5] A.M. Attiya, A. Safaai-Jazi, Simulation of Ultra-Wideband indoor propagation, Microwave and Optical Technology Letters 42 (2004).
[6] H. Sugahara, Y. Watanabe, T. Ono, K. Okanoue, S. Yamazaki, Development and experimental evaluations of RS-2000. A propagation simulator for UWB systems, in: IWUWBST, 2004.
[7] C.-N. Chuah, D.N.C. Tse, J.M. Kahn, R.A. Valenzuela, Capacity scaling in MIMO wireless under correlated fading, IEEE Transactions on Information Theory, vol. 48 (3), pp. 637–650.
[8] A. Shlivinski, E. Heyman, R. Kastner, Antenna characterization in the time domain, IEEE Transaction on Antenna and Propagation 45 (July 1997) 1140–1149.
[9] C. Roblin, S. Bories, A. Sibille, Characterization tools of antennas in the time domain, in: IWUWBS, 2003.
[10] W. Soergel, C. Waldschmidt, W. Wiesbeck, Antenna characterization for ultra wideband communications, in: IWUWBS, 2003.
[11] Y. Lo, S. Lee, Antenna Hanbook: Theorems and Formulas, Van Nostrand Reinhold, 1988 (Chapter 2).
[12] M.L. Morris, M.A. Jensen, Network model for MIMO systems with coupled antennas and noisy amplifiers, IEEE Transactions on Antenna and Propagation 53 (1) (January 2005) 545–552.
[13] F. Tchoffo Talom, Modélisation déterministe du canal de propagation indoor dans un contexte Ultra Wide Band, Ph.D. thesis, IETR/INSA, 2005.
[14] A. Derode, A. Tourin, J. de Rosny, M. Tanter, S. Yon, M. Fink, Taking advantage of multiple scattering to communicate with time reversal antennas, Physical Review Letters 90, pp. 465–497.
[15] R.C. Qiu, C. Zhou, N. Guo, J.Q. Zhang, Time reversal with MISO for ultra-wideband communications: Experimental results, in: IEEE Radio and Wireless Symposium, San Diego, 2006.